SCIENCE CHINA
Chemistry

• ARTICLES •
· SPECIAL TOPIC · Single-Molecule, Single-Particle and Single-Cell Bioimaging

October 2017 Vol.60 No.10: 1310–1317
doi: 10.1007/s11426-017-9072-5

Single-molecule imaging reveals the stoichiometry change of epidermal growth factor receptor during transactivation by β_2-adrenergic receptor

Mingliang Zhang[1,2], Kangmin He[1,2], Jimin Wu[1], Nan Li[2], Jinghe Yuan[2], Wei Zhou[2], Zi Ye[2], Zijian Li[1], Han Xiao[1], Zhizhen Lv[1], Youyi Zhang[1*] & Xiaohong Fang[2*]

[1]*Institute of Vascular Medicine of Third Hospital, Ministry of Health Key Laboratory of Cardiovascular Molecular Biology and Regulatory Peptides, Beijing Key Laboratory of Cardiovascular Receptors and Academy for Advanced Interdisciplinary Studies, Peking University, Beijing 100191, China*
[2]*Beijing National Laboratory for Molecular Sciences, Key Laboratory of Molecular Nanostructures and Nanotechnology, Institute of Chemistry, Chinese Academy of Sciences, Beijing 100190, China*

Received April 8, 2017; accepted April 25, 2017; published online July 4, 2017

Stimulation of G protein-coupled receptors (GPCRs) can lead to the transactivation of the epidermal growth factor receptors (EGFR). The cross-communication between the two signaling pathways regulates several important physiological or pathological processes. However, the molecule mechanism underlying EGFR transactivation remains poorly understood. Here, we aim to study the GPCR-mediated EGFR transactivation process using the single-molecule fluorescence imaging and tracking approach. We found that although EGFR existed as monomers at the plasma membrane of resting cells, they became dimers and thus diffused slower following the activation of β_2-adrenergic receptor (β_2-AR) by isoproterenol (ISO). We further proved that β_2-AR-mediated changes of EGFR in stoichiometry and dynamics were mediated by Src kinase. Thus, the observations obtained via the single-molecule imaging and tracking methods shed new insights into the molecular mechanism of EGFR transactivation at single molecule level.

transactivation, epidermal growth factor receptor (EGFR), β_2-adrenergic receptor (β_2-AR), single molecule imaging

Citation: Zhang M, He K, Wu J, Li N, Yuan J, Zhou W, Ye Z, Li Z, Xiao H, Lv Z, Zhang Y, Fang X. Single-molecule imaging reveals the stoichiometry change of epidermal growth factor receptor during transactivation by β_2-adrenergic receptor. *Sci China Chem*, 2017, 60: 1310–1317, doi: 10.1007/s11426-017-9072-5

1 Introduction

Transactivation is the process that receptors are activated by the stimulation of ligands of other receptors. It is a typical cross-communication between different cell signaling systems [1–3]. The transmembrane G protein-coupled receptors (GPCRs) and receptor-tyrosine kinases (RTKs), the two major classes of cell surface transmembrane proteins, transduce a variety of extracellular stimulus into intracellular signaling to regulate multiple cellular functions [4–8]. It has been observed that activation of GPCRs could lead to the activation of RTKs [9,10]. The cross-communication between the two signaling pathways regulates many physiological and pathological processes such as cell proliferation, tumor progression and development of cardiovascular diseases [11–14].

As a typical member of RTK family, epidermal growth factor receptors (EGFR) transactivation by β2-AR (a prototypical member of GPCRs) has been already documented [1,12,15,16]. However, the mechanism underlying this process remains poorly understood. Previous works have

*Corresponding authors (email: zhangyy@bjmu.edu.cn; xfang@iccas.ac.cn)

led to the identification of the ligand-dependent or -independent approaches in EGFR transactivation by GPCRs in different context. In the ligand dependent mechanism, stimulation of GPCRs via selective agonists triggers the membrane-bound matrix metalloproteases (MMPs)-mediated proteolytic cleavage of a Pro-Ligand, which generates a cleaved ligand EGF that binds to EGFR and induces signal transduction in an autocrine and paracrine manner [16–18]. The ligand-independent mechanism requires the activation of the intracellular protein Src to directly phosphorylates EGFR, but without the involvement of either MMP or EGF [9,11,12]. However, these previous studies based mainly on biochemical assays have difficulty in directly revealing of the spatial and temporal dynamics of EGFR in living cells during GPCRs-mediated transactivation [1,2,12,15]. Studying of receptor stoichiometry and dynamics properties before and after activation is of critical importance to understand the molecular mechanism of initial signaling complex formation. It is now well established that ligand EGF-induced EGFR dimer formation on cell surface is the initial, yet essential step during the classical EGFR activation and signaling process [19–21]. Thus, the direct observation the stoichiometry and dynamics properties of EGFR transactivation in living cells and in real time is expected to differentiate the two mechanisms and provide deeper insight into the molecule mechanism of receptor transactivation.

Single-molecule fluorescence imaging and single-particle tracking (SPT) has become an emerging technique to study the receptor stoichiometry and dynamics in living cells [22–26]. By optimizing the single-molecule imaging technique, we have studied and revealed the stoichiometry of transforming growth factor β receptors [27–29], β_2-AR [30] and EGFR [27,28] at the plasma membrane of resting or ligand-stimulated cells. The direct tracking of diffusion dynamics of single receptors at the plasma membrane helps to determine the stoichiometry, kinetics and interactions of signaling receptors during their normal activation and biased activation [30]. In this work, for the first time, we have applied the single-molecule total internal reflection fluorescence microscopy (TIRFM) imaging and SPT techniques to the study of transactivation. We are able to reveal the stoichiometry and dynamics of EGFR during its transactivation by β_2-AR, and clarify the role of Src in this transactivation.

2 Materials and method

2.1 Plasmids

The EGFR-EGFP plasmid was purchased from Addgene (Addgene plasmid 32751) [31], The β_2-AR-mcherry plasmid was constructed as described [30]. The plasmids were confirmed by DNA sequencing.

2.2 Cell culture and transfection

HeLa cells were cultured in DMEM (Gibco) supplemented with 10% fatal bovine serun (FBS; HyClone, USA) at 37 °C with 5% CO_2, then they were transfected with 0.2 ng/mL EGFR-EGFP or β_2-AR-mCherry in the serum- and phenol red-free DMEM (the minimal medium) using lipofectamine 2000 (Invitrogen, USA) according to manufacturer's instructions. After transfection for 6 h, the cells were imaged in the minimal medium using fluorescence microscopy.

For ligand stimulation, the cells were incubated with isoproterenol (ISO) (10^{-5} M, Sigma, USA) or EGF (10 ng/mL, R&D Systems) in the serum free medium for 15 min and then used for live cell imaging by TIRFM. For fixed cell imaging, the transfected cells were washed with phosphate buffered saline (PBS) for 3 times and fixed in 4% paraformaldehyde in PBS for 20 min, and then used for TIRFM imaging. HeLa cells were used for most imaging experiments unless specified.

2.3 Single molecule fluorescence imaging

Single molecule fluorescence imaging was performed on an objective-type TIRFM microscopy with a 100×/1.45NA Plan Apochromat objective (Olympus, Japan) and a 14-bit back-illuminated electron-multiplying charge-coupled device camera (EMCCD) (Andor iXon DU-897 BV) [25,27]. EGFP and mCherry tagged samples were excited at 488 and 561 nm line of lasers (Melles Griot, Carlsbad, CA, USA), respectively. The collected fluorescent signals were passed through the filter HQ 525/50 and 617/73 (Chroma Technology, USA) corresponding to 488 and 561 nm excitation, and then directed to an EMCCD camera. The gain of the EMCCD camera was set at 300. Movies of 300 frames were acquired for each sample at a frame rate of 10 Hz.

2.4 Single receptor detection and tracking

Single receptor molecules were detected and tracked using u-Track [32,33] as described in our previous study [25]. In brief, to characterize the diffusion rate of individual receptors, the positions of these individual receptors in each frame were firstly determined by detecting significant local intensity maxima and then fitted with a two-dimensional Gaussian function. Then these detected spots were linked and the trajectories of each receptor molecules were generated [25].

2.5 Image analysis

The fluorescence intensity distribution and photobleaching steps of single EGFR molecules at the cell membrane were analyzed according to the method we reported previously [27]. Colocalization of EGFR-EGFP and β_2-AR-mCherry

was determined using the JACoP ImageJ plugin as reported [34,35]. The background in the imaged was subtracted using the rolling ball method before the colocalization analysis.

To analyze the diffusion dynamics of EGFR on cell membrane, fluorescent trajectories lasting for at least 5 frames were collected for trajectory analysis as described [25,36]. The mean square displacement (MSD) was calculated with the following formula [37,38]:

$$\mathrm{MSD}(n\delta t) = \frac{1}{N-1-n}\sum_{i=1}^{N-1-n}\{[x(i\delta t+n\delta t)-x(i\delta t)]^2 +[y(i\delta t+n\delta t)-y(i\delta t)]^2\}$$

For each EGFR molecule, the diffusion coefficient (D) was calculated according to the equation MSD=4$D\Delta t$ using the first four spots in the MSD-Δt plot [25].

2.6 Silencing of Src expression

The control siRNA target sequence was 5'-AATTCTCCGAACGTGTCACGT-3'. The Src siRNA target sequence was 5′-TGTTCGGAGGCTTCAACTCCT-3' [39]. These RNA oligos were purchased from GenePharma Co. (Suzhou, China). Src knockdown was achieved by transfecting the cells with 100 pmol siRNA using Lipofectamine2000 (Invitrogen, USA) for 48 h. The knockdown efficiency was validated by both immunofluorescence and Western blot.

For immunofluorescence assays, the control and Scr-depleted HeLa cells were pretreated in PBS containing 0.5% Triton X-100 for 8 min, fixed with the same PBS buffer containing 4% formaldehyde for 25 min, and then incubated with Src antibody (Cell Signaling Technology, 1:200) at 4 °C over night and Alexa Fluor 488-conjugated secondary antibody (anti rabbit, Invitrogen, 1:400) for 1 h. The stained cells were imaged by a fluorescence confocal microscope (FV1000-IX81, Olympus, Japan) and a 100×/1.40NA objective was used.

2.7 Western blot analysis

Western blot analyses were performed as described in Ref. [14]. In brief, cell lysates were separated on 8% or 10% sodium dodecyl sulfate-polyacrylamide gelelectrophoresis (SDS-PAGE) and then transferred by electroblotting to a nitrocellulose membrane (Pall). Chemiluminescence detection was performed using the SuperECL reagent (Applygen, Beijing, China) and the GeneGnome Bio Imaging System (Syngene, UK). GAPDH was used as the loading control. Src was detected by immunoblotting with the anti-Src antibody (Cell Signaling Technology, 1:1000). EGFR and ERK were detected using antibodies specific for EGFR, P-EGFR, ERK and P-ERK (Cell Signaling Technology, USA).

2.8 Statistics analysis

For statistical analysis of samples with small sizes, the Student's *t*-tests were performed using GraphPad Prism (GraphPad Software). For robust single-molecule analysis, the Nonparametric Mann-Whiteney U test was used using GraphPad Prism (GraphPad Software). *p*-Value less than 0.05 was considered statistically significant.

3 Results and discussion

3.1 EGFR molecules underwent dimerization during β_2-AR-mediated EGFR transactivation

Single molecule fluorescence imaging was used to study the stoichiometry of EGFR during transactivation by β_2-AR. HeLa cells transfected with EGFR-EGFP were imaged using TIRFM calibrated with single EGFP molecule sensitivity. The cells were imaged 6 h after transfection to ensure EGFR-EGFP molecules were expressed at low density (0.075–0.25 particle/μm^2 ensuring the single-molecule EGFR distribution within the spatial resolution of microscopy [27]). As shown in the representative TIRFM image (Figure 1(a)), EGFR-EGFP molecules appeared as well-dispersed diffraction-limited fluorescent spots (5×5 pixels) at the plasma membrane and then got photobleached in a stepwise way (Figure 1(b)). The stoichiometry of EGFP-fused membrane-bound proteins can be determined by analyzing their fluorescence intensity distribution [27,28] and photobleaching steps [27,40]. We found that the fluorescence intensity distribution of individual EGFP-tagged EGFR molecules exhibited a sum of two Gaussian distributions (Figure 1(c)), with the value of the first peak intensity which covering the majority of the spots close to that of single purified EGFP molecules attached to coverslips and the second peak with the intensity of twice as the first one, suggesting that they were monomers and dimers respectively. In cells without stimulation, 85% of EGFR-EGFP molecules were monomers and 15% were dimers.

The photobleaching steps of individual fluorescent EGFR-EGFP molecules were analyzed with our newly developed algorithm which could determine the photobleaching steps of more than thousands of EGFR-EGFP molecules automatically [30,41]. The results showed that 91.1% of EGFR-EGFP molecules were monomers and 8.5% were dimers in the resting cells (Figure 1(f)). Therefore, our study supports the view that EGFR exists mainly as monomers at the basal state [42].

We then examined the effect of the β_2-AR agonist ISO on EGFR dimerization during transactivation, as well as EGFR cognate ligand EGF. Western blot analysis confirmed that ISO could effectively activate EGFR in our system (Figure S1(a, b), Supporting Information online). Consistent with the previous reports [1,12], ISO stimulation resulted in increased phosphorylation of EGFR and its downstream target extracellular-regulated kinase (Erk)

Next, we investigated the stoichiometry of EGFR-EGFP in

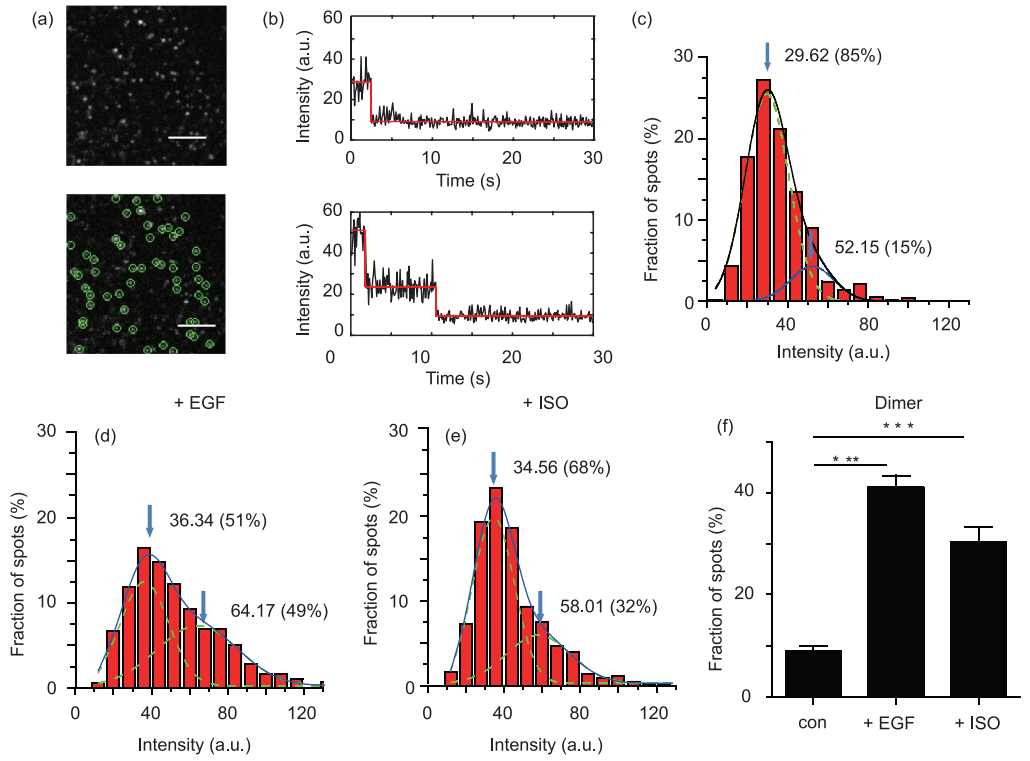

Figure 1 β_2-AR agonist isoproterenol (ISO) induced EGFR-EGFP dimerization. (a) A representative single-molecule image (top panel) shows the distribution of EGFR-EGFP molecules at the plasma membrane of a HeLa cell imaged by TIRFM. The image was generated by averaging the first five frames of a movie and then the background was subtracted. The diffraction-limited spots enclosed with green circles (5×5 pixel) represented the detected individual EGFR-EGFP molecules (bottom panel). Scale bar, 5 μm. (b) Two representative time courses of EGFR-EGFP emission showed one- and two-step bleaching respectively. The red lines denote the automatically estimated bleaching steps. (c) Distribution of the fluorescence intensity of diffraction-limited EGFR-EGFP spots (n=1758 from 24 cells). The curves show the fitting of a Gaussian function and the two peaks represent the intensity of EGFR-EGFP monomer and dimer, respectively. Correlation coefficient (R) of the Gaussian fitting is 0.98. The arrowheads indicate the peak positions of the fitting curves. Numbers in the parentheses are the fractions of monomer and dimer. (d, e) Distribution of the fluorescence intensity of individual EGFR-EGFP molecules from the cells treated with (d) EGF (10 ng/mL, n=1228 from 15 cells) or (e) ISO (10^{-5} M, n=1173 from 16 cells). (f) Frequency of two-step bleaching events for EGFR-EGFP in resting and drug stimulated cells. Data represent mean ±S.E.M from 10 cells each. *** p<0.001 (color online).

cells treated with either ISO for transactivation or EGF as a control. After treating the cells with 10 ng/mL EGF, the histogram of the fluorescent intensities of single EGFR-EGFP molecules showed a distribution with 51% monomers and 49% dimers (Figure 1(d)). The photobleaching step analysis also showed that the dimer population of EGFR-EGFP increased to 40.23% after EGF stimulation (Figure 1(f)). More importantly, the dimer population of EGFR-EGFP molecules showed a significant increase from 15% to 32%, while the monomer population decreased from 85% to 68% by ISO transactivation (Figure 1(e)). The photobleaching step analysis also showed that the dimer population of EGFR-EGFP increased to 27.99% after transactivation by ISO (Figure 1(f)).

Therefore, by the single-molecule fluorescence imaging tool, we have demonstrated that similar to EGF, the β_2-AR agonist ISO could increasing EGFR dimerization during EGFR transactivation.

3.2 Diffusion dynamics of EGFR during β_2-AR-mediated transactivation

The diffusion dynamics of signaling receptors at the plasma membrane have been suggested to be involved in cell signaling activation and transduction [19–21,24,43,44]. We next studied the diffusion dynamics of the single transactivated EGFR at the plasma membrane by live-cell single-molecule and SPT [25]. By tracking thousands of randomly diffused individual EGFR-EGFP molecules, we quantified the diffusion rate of EGFR-EGFP molecules. EGF stimulation shifted the diffusion coefficients (D) of EGFR molecules toward lower values, i.e., from 0.077 μm^2/s in unstimulated cells to 0.036 μm^2/s in stimulated cells (Figure 2, p<0.001). Importantly, ISO stimulation slowed down EGFR diffusion, with the diffusion coefficient reduced from 0.077 to 0.052 μm^2/s (Figure 2, p<0.001). Since the diffusion coefficient of membrane bound proteins is related to their sizes [45], the slower diffusion of EGFR indicates the higher order oligomerization (e.g. dimer) of EGFR induced by ISO.

Of note, ISO induced slowdown of EGFR diffusion was smaller than that of EGF, which is consistent with the relatively less dimers in cells treated with ISO than cells treated with EGF (Figure 1(f)). Taken together, these data have pro-

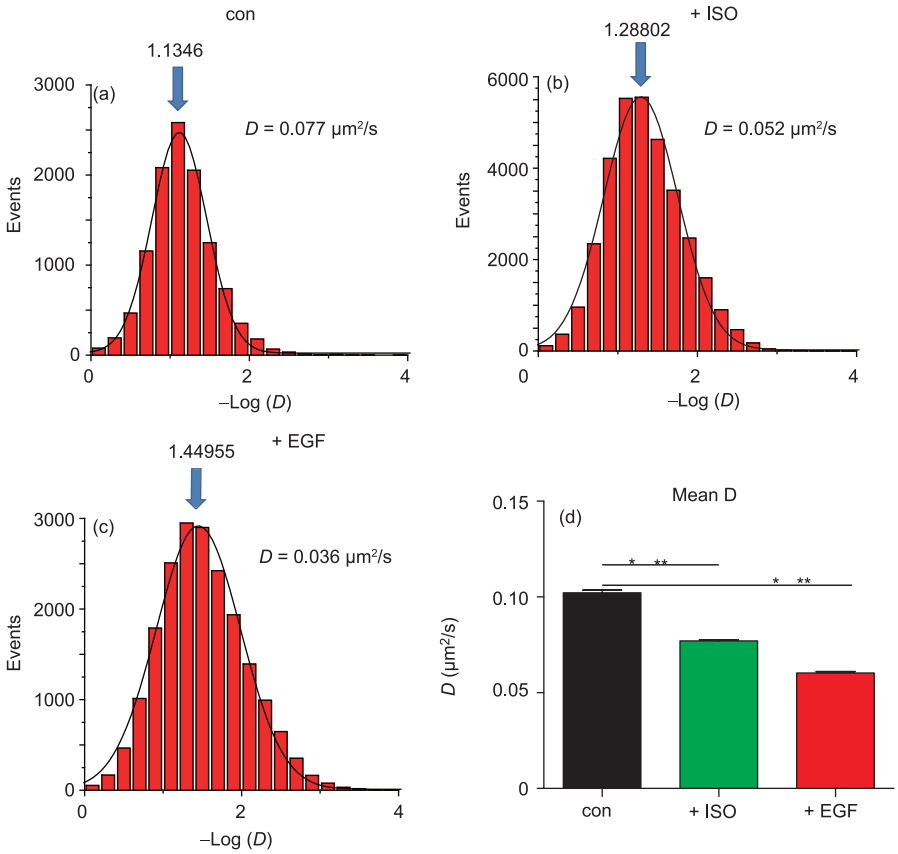

Figure 2 Diffusion dynamics of EGFR-EGFP at the plasma membrane of cells treated without or with stimulation revealed by TIRFM imaging and single particle tracking. Diffusion rates *D* of membrane-docked EGFR-EGFP molecules in (a) resting HeLa cells (n=12 cells), or HeLa cells stimulated with (b) EGF (n=9 cells) or (c) ISO (n=10 cells). The *D* values from the two groups (a, c) are significantly different (p<0.001, Mann-Whiteney U test). (d) The average value of diffusion rate of thousands molecules from (a–c). The data are presented as means ± S.E.M. *** p<0.001 (color online).

ved that EGFR molecules undergo slower diffusion during β_2-AR-mediated transactivation.

3.3 Src kinase was involved in EGFR dimerization during transactivation by β_2-AR

Two different mechanisms, the ligand-dependent and -independent mechanisms, have been proposed to explain GPCRs-mediated in EGFR transactivation. The ligand-independent mechanism requires the activation of the tyrosine kinase Src [1,12]. Since the single molecule imaging approach we used here could directly monitor the early effects (dimerization and diffusion) of EGFR transactivation by GPCR, we then started to investigate the potential role of Src during β_2-AR-mediated transactivation. We used two approaches to interfere Src function, either by treated the cells with Src specific inhibitor PP2 or by depleting Scr expression by siRNA (Figure S2(a, b)). We found that pre-treatment with PP2 (1 μM for 30 min) prevented ISO-induced EGFR dimer formation (Figure 3(a–d)). Similarly, knocking down the expression of Scr attenuated ISO-induced EGFR dimer formation (Figure 3(e, f)). These results proved that the dimerization of EGFR during β_2-AR-induced transactivation was regulated by Src.

3.4 EGFR did not co-localize with β_2-AR during transactivation at the cell membrane

By using co-immunoprecipitation or confocal microscopy, it has been shown that β_2-AR-mediated EGFR transactivation required the formation of β_2-AR-EGFR complex [1,16,46]. We also confirmed the colocalzation of β_2-AR and EGFR in endocytic carries and endosomes inside the cells after ISO stimulation by confocal imaging (Figure S3). The question remains whether the activated individual EGFR and β_2-AR molecules form complex right after their activation at cell surface, before their enrichment and thus colocalization in clathrin-coated pits/vesicles.

By imaging the cells co-expressing EGFR-EGFP and β_2-AR-mCherry at the low expression level using TIRFM, we found that the majority of individual EGFR molecules did not colocalize with individual β_2-AR molecules (Figure 4). Although ISO stimulation increased the dimer formation of both EGFR (Figure 1) and β_2-AR [30,41], the co-localization between individual EGFR-EGFP and β_2-AR-mCherry molecules did not increase. In the previous reports that using traditional biochemical assays [1,16,46], it is hard to distinguish whether the co-localization of these receptors

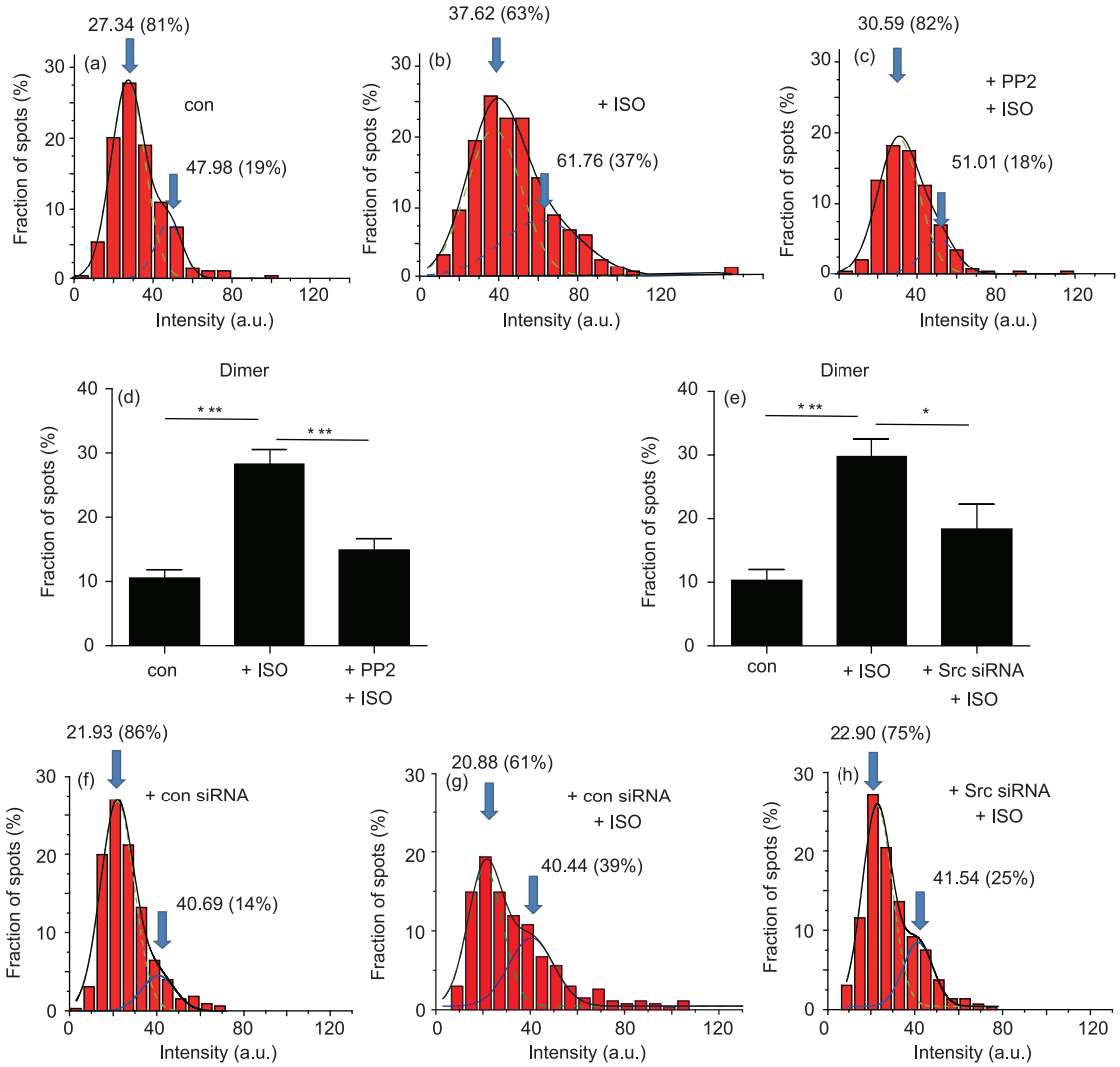

Figure 3 Src regulated EGFR-EGFP dimerization during transactivation by β_2-AR. (a–c) Distribution of the fluorescence intensity of individual EGFR-EGFP spots in control cells (a), ISO-stimulated cells (b), and cells pre-treated for 30 min with Src inhibitor PP2 (1 μM) and then stimulated with ISO (c). (d) Frequency of two-step bleaching events for EGFR-EGFP in control and drug stimulated cells. (e) Frequency of two-step bleaching events for EGFR-EGFP in the cells transfected with the control siRNA or siRNA targeting Scr, and then treated with ISO as indicated. The data are presented as means ±S.E.M. * p<0.05 and *** p<0.001. (f–h) Distribution of the fluorescence intensity of individual EGFR-EGFP spots in the cells transfected with the control siRNA or siRNA targeting Scr, and then treated with ISO as indicated (color online).

occurred in cytoplasm or on cell membrane. With our TIRFM based single-molecule method only imaging the molecular event on plasma membrane, interaction of the two receptors can be observed on the cell membrane at single-molecule level right after activation. Our result suggests that the transactivation of EGFR by β_2-AR is not induced by direct interaction between the two types of receptors during the early stages of ligand stimulation, but instead, it is regulated by the Scr kinase dependent EGFR dimerization, and the dimerization of EGFR results in EGFR phosphorylation and activation.

In present study, by employing single-molecule fluorescence imaging and single partial tracking method, we have revealed the stoichiometry change of EGFR during transactivation. As we known, the previously proposed ligand-independent mechanisms of transactivation involve the activation of Src family proteins, the downstream protein of β_2-AR signaling pathway, and then the direct mediation of EGFR phosphorylation in its cytosolic domain without detectable EGF-like ligands. On the other hand, EGF induced EGFR dimerization is a general approach for the normal EGFR activation as EGFR dimerization leads to its phosphorylation and signaling. Since there is no EGF ligand release during the ligand-independent transactivation, it is unclear whether EGFR would dimerize to promote its activation or not in this process. In this work, we found that EGFR became dimers and diffused slower following the ISO stimulated transactivation. The dimerization of EGFR during transactivation is regulated by Src. Moreover, the transactivation of EGFR by β_2-AR did not involve direct interaction between the two receptors on the cell membrane. Therefore, our results suggest

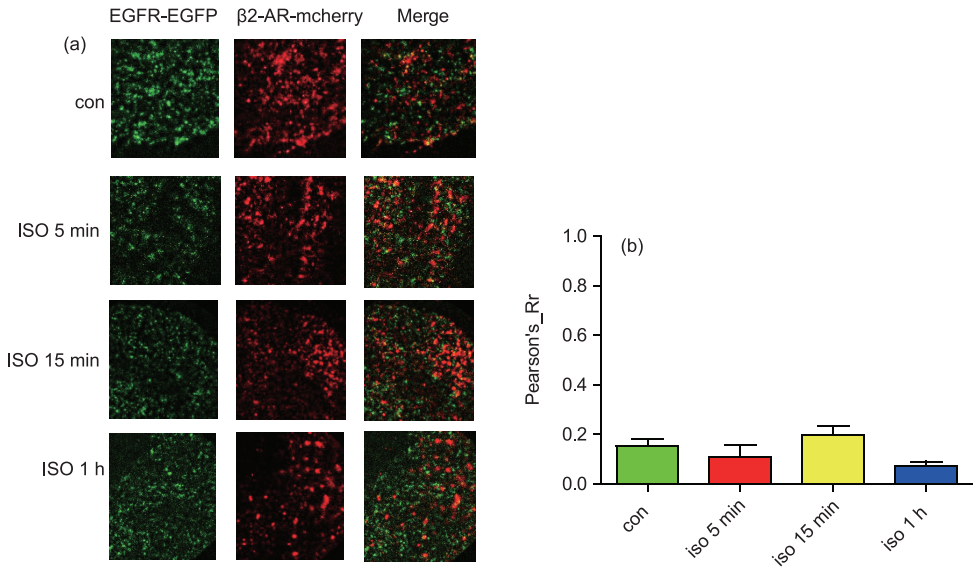

Figure 4 EGFR-EGFP did not colocalized with β_2-AR-mCherry at the plasma membrane of cells stimulated by ISO. (a) HeLa cells were co-expressed with β_2-AR-mcherry and EGFR-EGFP for 6 h and then imaged by dual-color TIRFM before and after ISO stimulation.(b) Quantification of the colocalization of β_2-AR-mCherry with EGFR-EGFP. The results are shown as means ±S.E.M of 6–10 cells (color online).

the possible approach of EGFR transactivation by Scr regulated EGFR dimerization and phosphorylation.

4 Conclusions

In conclusion, with single-molecule fluorescence imaging and single-particle tracking, we are able to directly study the GPCR-mediated EGFR transactivation process at single molecule/receptor level. We found the β_2-AR activation resulted in the dimer formation and slower diffusion of EGFR. We further proved that this process was mediated by Scr. It provides new insight into the understanding of the mechanism of GPCR-mediated EGFR transactivation. Our study also presents a new approach of studying receptor transactivation by the single-molecule fluorescence imaging.

Acknowledgments This work was supported by the National Basic Research Program of China (2013CB933701), the National Natural Science Foundation of China (81530009, 21127901, 91213305), and Chinese Academy of Science.

Conflict of interest The authors declare that they have no conflict of interest.

Supporting information The supporting information is available online at http://chem.scichina.com and http://link.springer.com/journal/11426. The supporting materials are published as submitted, without typesetting or editing. The responsibility for scientific accuracy and content remains entirely with the authors.

1 Maudsley S, Pierce KL, Zamah AM, Miller WE, Ahn S, Daaka Y, Lefkowitz RJ, Luttrell LM. *J Biol Chem*, 2000, 275: 9572–9580
2 Daub H, Ulrich Weiss F, Wallasch C, Ullrich A. *Nature*, 1996, 379: 557–560
3 Cattaneo F, Guerra G, Parisi M, De Marinis M, Tafuri D, Cinelli M, Ammendola R. *Int J Mol Sci*, 2014, 15: 19700–19728
4 Rockman HA, Koch WJ, Lefkowitz RJ. *Nature*, 2002, 415: 206–212
5 Lymperopoulos A, Rengo G, Koch WJ. *Circ Res*, 2013, 113: 739–753
6 Yarden Y, Sliwkowski MX. *Nat Rev Mol Cell Biol*, 2001, 2: 127–137
7 Wang T. *Sci China Chem*, 2013, 56: 1344–1350
8 Wang SC, Sun M, Zhang YM, Zhang J, He LC. *Sci China Chem*, 2010, 53: 2357–2362
9 Wang Z. *Int J Mol Sci*, 2016, 17: 95
10 Forrester SJ, Kawai T, O'Brien S, Thomas W, Harris RC, Eguchi S. *Annu Rev Pharmacol Toxicol*, 2016, 56: 627–653
11 Almendro V, Garcia-Recio S, Gascon P. *Curr Drug Targets*, 2010, 11: 1169–1180
12 Drube S, Stirnweiss J, Valkova C, Liebmann C. *Cell Signal*, 2006, 18: 1633–1646
13 Fischer OM, Hart S, Gschwind A, Ullrich A. *Biochm Soc Trans*, 2003, 31: 1203–1208
14 Li Y, Zhang H, Liao W, Song Y, Ma X, Chen C, Lu Z, Li Z, Zhang Y. *Am J Physiol Heart Circ Physiol*, 2011, 301: H1941–H1951
15 Noma T, Lemaire A, Naga Prasad SV, Barki-Harrington L, Tilley DG, Chen J, Le Corvoisier P, Violin JD, Wei H, Lefkowitz RJ, Rockman HA. *J Clin Invest*, 2007, 117: 2445–2458
16 Watson LJ, Alexander KM, Mohan ML, Bowman AL, Mangmool S, Xiao K, Naga Prasad SV, Rockman HA. *Cell Signal*, 2016, 28: 1580–1592
17 Prenzel N, Zwick E, Daub H, Leserer M, Abraham R, Wallasch C, Ullrich A. *Nature*, 1999, 402: 884–888
18 Kim IM, Tilley DG, Chen J, Salazar NC, Whalen EJ, Violin JD, Rockman HA. *Proc Natl Acad Sci USA*, 2008, 105: 14555–14560
19 Jorissen RN, Walker F, Pouliot N, Garrett TPJ, Ward CW, Burgess AW. *Exp Cell Res*, 2003, 284: 31–53
20 Sako Y, Minoghchi S, Yanagida T. *Nat Cell Biol*, 2000, 2: 168–172
21 Lemmon MA, Schlessinger J. *Cell*, 2010, 141: 1117–1134
22 Chen C. *Sci Bull*, 2015, 60: 1787–1788
23 Cheng M, Zhang W, Yuan J, Luo W, Li N, Lin S, Yang Y, Fang X, Chen PR. *Chem Commun*, 2014, 50: 14724–14727
24 Chung I, Akita R, Vandlen R, Toomre D, Schlessinger J, Mellman I. *Nature*, 2010, 464: 783–787

25 Li N, Yang Y, He K, Zhang F, Zhao L, Zhou W, Yuan J, Liang W, Fang X. *Sci Rep*, 2016, 6: 33469
26 Yang Y, Xu Y, Xia T, Chen F, Zhang C, Liang W, Lai L, Fang X. *Chem Commun*, 2011, 47: 5440–5442
27 Zhang W, Jiang Y, Wang Q, Ma X, Xiao Z, Zuo W, Fang X, Chen YG. *Proc Natl Acad Sci USA*, 2009, 106: 15679–15683
28 He K, Fu Y, Zhang W, Yuan J, Li Z, Lv Z, Zhang Y, Fang X. *Biochem Biophys Res Commun*, 2011, 407: 313–317
29 Ye Z, Li N, Zhao L, Sun Y, Ruan H, Zhang M, Yuan J, Fang X. *Sci Bull*, 2016, 61: 632–638
30 Sun Y, Li N, Zhang M, Zhou W, Yuan J, Zhao R, Wu J, Li Z, Zhang Y, Fang X. *Chem Commun*, 2016, 52: 7086–7089
31 Carter RE, Sorkin A. *J Biol Chem*, 1998, 273: 35000–35007
32 Jaqaman K, Loerke D, Mettlen M, Kuwata H, Grinstein S, Schmid SL, Danuser G. *Nat Meth*, 2008, 5: 695–702
33 Shuang B, Byers CP, Kisley L, Wang LY, Zhao J, Morimura H, Link S, Landes CF. *Langmuir*, 2013, 29: 228–234
34 Klein ME, Younts TJ, Castillo PE, Jordan BA. *Proc Natl Acad Sci USA*, 2013, 110: 3125–3130
35 Adler J, Parmryd I. *Cytometry*, 2010, 77A: 733–742
36 Calebiro D, Rieken F, Wagner J, Sungkaworn T, Zabel U, Borzi A, Cocucci E, Zürn A, Lohse MJ. *Proc Natl Acad Sci USA*, 2013, 110: 743–748
37 Habuchi S, Fujiwara S, Yamamoto T, Vacha M, Tezuka Y. *Anal Chem*, 2013, 85: 7369–7376
38 Kusumi A, Sako Y, Yamamoto M. *Biophys J*, 1993, 65: 2021–2040
39 Bjorge JD, Pang AS, Funnell M, Chen KY, Diaz R, Magliocco AM, Fujita DJ. *PLoS ONE*, 2011, 6: e19309
40 Ji W, Xu P, Li Z, Lu J, Liu L, Zhan Y, Chen Y, Hille B, Xu T, Chen L. *Proc Natl Acad Sci USA*, 2008, 105: 13668–13673
41 Yuan J, He K, Cheng M, Yu J, Fang X. *Chem Asian J*, 2014, 9: 2303–2308
42 Huang Y, Bharill S, Karandur D, Peterson SM, Marita M, Shi X, Kaliszewski MJ, Smith AW, Isacoff EY, Kuriyan J. *eLife*, 2016, 5: e14107
43 Low-Nam ST, Lidke KA, Cutler PJ, Roovers RC, van Bergen en Henegouwen PMP, Wilson BS, Lidke DS. *Nat Struct Mol Biol*, 2011, 18: 1244–1249
44 Jaqaman K, Kuwata H, Touret N, Collins R, Trimble WS, Danuser G, Grinstein S. *Cell*, 2011, 146: 593–606
45 Gambin Y, Lopez-Esparza R, Reffay M, Sierecki E, Gov NS, Genest M, Hodges RS, Urbach W. *Proc Natl Acad Sci USA*, 2006, 103: 2098–2102
46 Tilley DG, Kim IM, Patel PA, Violin JD, Rockman HA. *J Biol Chem*, 2009, 284: 20375–20386